

TORSIONAL VIBRATION REDUCTION IN INTERNAL COMBUSTION ENGINES USING CENTRIFUGAL PENDULUMS

Cheng-Tang Lee
Steven W. Shaw

**Department of Mechanical Engineering
Michigan State University
East Lansing, MI48824**

ABSTRACT

The goal of the present work is to investigate the performance of tautochronic centrifugal pendulum vibration absorbers (CPVA's) for reducing torsional vibration in internal combustion engines. A mathematical model is first built for the torsional dynamics of an in-line, four-stroke, four-cylinder engine, including the consideration of inertia effects of connecting rods and pistons, gas pressure inside the cylinder chambers, and friction in bearings. Three configurations of the tautochronic CPVA are applied to the model, including (1) a single CPVA tuned to order 2, (2) a pair of CPVA's tuned to order 1, (3) two CPVA's, in which one is tuned to order 2 while the other is tuned to order 4. The moment of inertia for all three configurations is kept constant for purposes of comparison. Numerical simulations are accomplished in order to evaluate the performance of each configuration. This preliminary study indicates that Configuration (3) offers the best result for minimizing the peak value of crankshaft angular acceleration.

1 INTRODUCTION

Centrifugal pendulum vibration absorbers (CPVA's) are used to reduce torsional oscillations in rotating and reciprocating machinery. They have the special property of being able to counteract applied torques of a given order over a range of operating speeds and torque amplitudes, and have been successfully employed in internal combustion engines and helicopter rotors. The history of these devices goes back several decades; Chapter XXX of the treatise by Ker Wilson (1968) provides a detailed history, describes several specific hardware implementations, and demonstrates many examples.

The basic operation of a CPVA is as follows. An absorber mass is driven by the centrifugal field of the crankshaft rotational motion in such a manner that its center of mass is restricted to move along a prescribed path. The motion of this mass provides a torque which can be designed to counteract a given disturbance torque, thus smoothing out torsional vibrations. In many applications, the disturbance torque is approximately a pure harmonic with a frequency n times that of the nominal rotation rate, Ω . Such a torque

is referred to as a torque of *order* n . The linear tuning of the CPVA for a torque of order n is accomplished by fixing at a particular value the curvature of the absorber path in the neighborhood of its operating point.

For nonlinear designs of the CPVA, the entire absorber path is specified. This is realized in industrial applications by the introduction of a bifilar design. Several paths have been employed, among which a certain epicycloid is known to be the *tautochrone* (constant frequency of oscillation) for a radial centrifugal field, as is present in rotating systems (Denman, 1985). This motivated a study, sponsored by Ford Motor Company, in which epicycloidal paths were used for absorbers implemented on an experimental four-cylinder, in-line, four-stroke engine. The papers by Denman (1992), Cronin (1992) and Borowski et al. (1991) describe various aspects of this effort.

The tautochrone offers a desirable harmonic response for the absorber mass in the case in which the crankshaft speed is held constant. However, the torque it produces contains higher harmonics which are induced by nonlinear kinematic effects. These become significant even at moderate amplitudes, causing distortion of the torque and reducing the effectiveness of the CPVA (see Shaw and Lee, 1994). In fact, it can be shown that a single absorber path cannot produce a purely single harmonic torque, and thus one must sustain the amplified higher harmonics unless some other steps are taken. Some possible remedies for confronting these higher order torques are the following: One can employ CPVA's tuned to the troublesome higher orders (as done in the study by Borowski et al., 1991), or one can employ the subharmonic absorber system recently developed by the authors (Lee et al., 1994). This latter arrangement makes use of the subharmonic response of a system consisting of a pair of identical absorbers which are tuned to $\frac{n}{2}$. This latter system has the desired properties for producing a purely harmonic torque.

The goal of the present work is to investigate the performance of various arrangements of tautochronic CPVA's on an internal combustion engine. A mathematical model is built for an in-line, four-stroke, four-cylinder engine, including inertia effects of connecting rods and pistons, the gas pressure inside the cylinder chambers, and friction in bearings. Three configurations of the tautochronic CPVA

are applied to the model, including (1) a single CPVA tuned to order 2, (2) a pair of CPVA's tuned to order 1, (3) two CPVA's in which one is tuned to order 2 and the other is tuned to order 4. The moment of inertia for all three configurations is kept constant for purposes of comparison. Numerical simulations are accomplished in order to evaluate the performance of each configuration.

This paper is organized as the following: Section 2 derives the equations of motion and explains the sources of speed fluctuations of the system. Section 3 shows results of the numerical simulations, and the paper closes in Section 4 with a brief discussion.

2 MODEL AND EQUATIONS OF MOTION

The system consists of a four-cylinder engine with N absorbers, and a flywheel attached to the crankshaft. Torsional vibrations of a rigid crankshaft are considered. The engine is a typical in-line, four-stroke, four-cylinder engine, in which the firing order of the engine is assumed to be 1-4-3-2 such that each cylinder leads the next firing cylinder by a phase of π . Connecting rod/piston assemblies are attached to the crankshaft at the usual phases for a four-cylinder engine (two each at a phase difference of π). The crankshaft is driven by combustion-induced gas pressure in the cylinders. The derivation of the equations of motion for this system involves the calculation of the kinetic energy of the whole system, and the determination of terms arising from viscous friction sources and the gas pressure. The equations are then obtained by applying the Lagrangian method.

The total kinetic energy of the system is obtained by summing over the individual cylinders, and adding the kinetic energy of the absorbers and the crankshaft/flywheel assembly. A schematic diagram of the second cylinder is shown in Figure 1, in which the symbols l_1 , l_2 , l_3 , l_4 , and l represents the lengths indicated, while the J_i 's represent various connecting joints. It is worth noting that the ratio between l_1 and l_2 is an important factor in design, and $k_1 = \frac{l_1}{l_2} < \frac{1}{3}$ in most real applications (Taylor, 1985). The symbols m_{b1} , m_{b2} , and m_p denote the effective masses of the crank throw, the connecting rod, and the piston, respectively, while I_{b1} and I_{b2} are the the moments of inertia of the crank throw and the connecting rod about their corresponding centers of mass, respectively. The forces acting on the assembly are $P(\theta)$ and F_s , the gas pressure and side forces acting on the piston, respectively, and F_v and F_h , the vertical and horizontal forces acting on the crankshaft by the main bearings.

For the given firing order (1-4-3-2), the angular displacement of the first, third, and fourth cylinders are $\theta + 3\pi$, $\theta + \pi$, and $\theta + 2\pi$, respectively, while θ denotes the angular orientation of the second cylinder. The kinetic energy of the engine is obtained by summing those of the flywheel/crankshaft and the four cylinders, thus yielding

$$T_E = \frac{1}{2} \vartheta(\theta) \Omega^2 \dot{\theta}^2, \quad (1)$$

where Ω is the nominal mean rotation rate of the engine, $(\dot{\cdot}) = \frac{d(\cdot)}{d\tau}$, $\tau = \Omega t$,

$$\vartheta(\theta) = I_4 + I_5 \sin^2 \theta + \frac{(I_6 + I_7 \sin^2 \theta) \cos^2 \theta}{1 - k_1^2 \sin^2 \theta}, \quad (2)$$

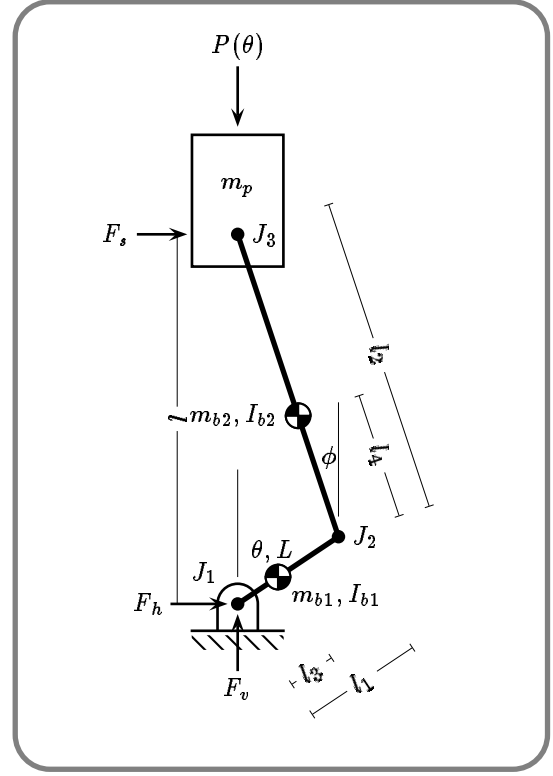


FIGURE 1: SCHEMATIC DIAGRAM OF ONE PISTON ASSEMBLY: THE SECOND CYLINDER OF AN IN-LINE, FOUR-STROKE, FOUR-CYLINDER ENGINE.

$$\begin{aligned} k_2 &= \frac{l_4}{l_2}, \\ I_4 &= I_f + 4\{I_{b1} + m_{b1}l_3^2 + m_{b2}l_1^2[1 - k_2(2 - k_2)]\}, \\ I_6 &= 4k_1^2 I_{b2}, \\ I_5 &= 4[m_p l_1^2 + m_{b2}k_2(2 - k_2)l_1^2], \\ I_7 &= 4k_1^2 l_1^2 (k_2^2 m_{b2} + m_p), \end{aligned} \quad (3)$$

and I_f is the moment of inertia of the crankshaft/flywheel assembly.

The i th absorber is modeled as a rigid body with a mass of m_i and a moment of inertia I_{ei} about its center of mass. A systematic diagram of it is shown in Figure 2. The center of mass moves along a path which is specified by $R_i = R_i(S_i)$, where R_i denotes the distance of a point on the i th absorber path to point O , and S_i is the arc length variable along the path. The variable S_i is also used to specify the location of m_i during it's motion. In bifilar form the absorber mass undergoes pure translation relative to the crankshaft. The value of R_i increases as one traverses from one end of the path up to a point Q_i , and then decreases until the other end is reached. Point Q_i is the vertex of the path. The path variable S_i is chosen such that $S_i = 0$ at point Q_i . Therefore, R_i reaches its maximum at $S_i = 0$, that is, $R_{oi} = \max R_i = R_i(0)$. The absorber has a nominal moment of inertia $I_i = m_i R_{oi}^2$ with respect to point O . With the addition of the kinetic energy of the absorbers, the total

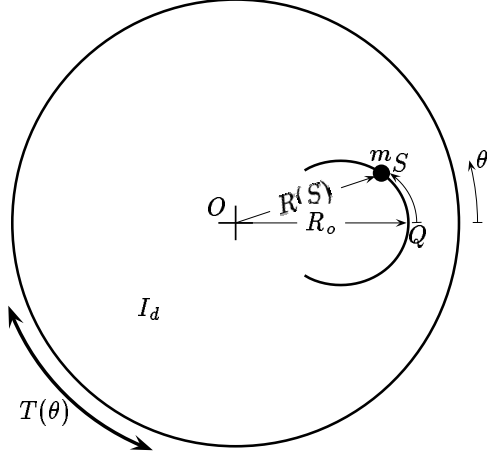


FIGURE 2: SCHEMATIC DIAGRAM OF A SINGLE ABSORBER AS A POINT MASS RIDING ON A SPECIFIED PATH.

kinetic energy of the complete system is given by

$$\text{K.E.} = \frac{1}{2}\vartheta(\theta)\Omega^2\dot{\theta}^2 + \frac{1}{2}\sum_{i=1}^N \{I_{ei}\dot{\theta}^2 + m_i [X_i(S_i)\dot{\theta}^2 + \dot{S}_i^2 + 2G_i(S_i)\dot{S}_i\dot{\theta}]\} \Omega^2, \quad (4)$$

where

$$X_i(S_i) = R_i^2(S_i), \quad G_i(S_i) = \sqrt{X_i(S_i) - \frac{1}{4}\left(\frac{dX_i}{dS_i}(S_i)\right)^2}. \quad (5)$$

The addition of the I_{ei} 's is treated as an increase in the crankshaft/flywheel inertia such that their effects can be absorbed by replacing $\vartheta(\theta)$ by $\vartheta(\theta) + \sum_{i=1}^N I_{ei}$.

The forcing terms acting on the crankshaft are separated into those caused by explosions in the cylinder chambers, those induced by friction, and a load on the crankshaft. Let $P(\theta)$ denote the gas pressure force acting on the second piston. The pressure $P(\theta)$ is 4π periodic, due to the nature of a four-stroke engine. To simplify further calculations, it is desirable to define the following two combinations of $P(\theta)$:

$$\begin{aligned} P_o(\theta) &= P(\theta) - P(\theta + \pi) + P(\theta + 2\pi) \\ &\quad - P(\theta + 3\pi), \\ P_e(\theta) &= P(\theta) + P(\theta + \pi) + P(\theta + 2\pi) \\ &\quad + P(\theta + 3\pi). \end{aligned} \quad (6)$$

Note that the forces, P_o and P_e , inherit the following symmetries:

$$P_o(\theta) = -P_o(\theta + \pi) \quad \text{and} \quad P_e(\theta) = P_e(\theta + \pi) \quad (7)$$

from the nature of $P(\theta)$. As a result, the fundamental periods of $P_o(\theta)$ and $P_e(\theta)$ are 2π and π , respectively. The net torque acting on the crankshaft from the gas pressures from all cylinders is given by

$$T(\theta) = l_1 \sin \theta \left(P_o(\theta) + \frac{k_1 P_e(\theta) \cos \theta}{\sqrt{1 - k_1^2 \sin^2 \theta}} \right), \quad (8)$$

which is periodic with respect to θ with a period of π .

The effects of friction can be divided into those from the various bearings and those from the absorbers. Friction from the bearings provides a net resistive torque on the crankshaft, but does not affect the motion of the absorbers directly. Assume that the friction forces are of linear viscous type, and that the corresponding joints J_1, J_2, J_3 , and the cylinder walls for different cylinders have the same damping factors, c_1, c_2, c_3 , and c_4 , respectively. The net torque generated by friction is then given by

$$- \left[c_5 + c_7 \sin^2 \theta \frac{(c_6 + c_7 k_1^2 \sin^2 \theta) \cos^2 \theta}{1 - k_1^2 \sin^2 \theta} \right] \Omega \dot{\theta}, \quad (9)$$

where

$$c_5 = 4(c_1 + c_2), \quad c_6 = 4k_1^2(c_2 + c_3), \quad c_7 = 4c_4 l_1^2.$$

The absorber damping also contributes a torque to the crankshaft given by $c_{ai}\Omega G_i(S_i)\dot{S}_i$, and applies a resistance force to the motion of the i th absorber of $-c_{ai}\Omega\dot{S}_i$, where c_{ai} is the corresponding damping coefficient.

To obtain the equations of motion, the procedure involves collecting together the kinetic energy terms given in equation (4) and the torques given in equations (8) and (9), the forces arising from absorber damping, a constant load torque T_o to maintain engine speed, and then applying Lagrange's method. It is desirable to nondimensionalize the equations of motion and to switch the independent variable from τ to θ . The latter change is helpful in realizing the dynamics of the system with respect to the crankshaft orientation. The nondimensionalization and some definitions of terms are as follows: $s_i = \frac{S_i}{R_{oi}}, r_i = \frac{R_i}{R_{oi}}, x_i(s_i) = \frac{X_i(R_{oi}s_i)}{R_{oi}^2}, g(s_i) = \frac{G(R_{oi}s_i)}{R_{oi}}, y = \frac{d\theta}{d\tau}, I_i = m_i R_{oi}^2, b_o(\theta) = \frac{\vartheta(\theta)}{I_f}, b_i = \frac{I_i}{I_f}, \hat{\mu}_{ai} = \frac{c_{ai}}{m_i \Omega}, \Gamma_o = \frac{T_o}{I_f \Omega^2}, \Gamma(\theta) = \frac{T(\theta)}{I_f \Omega^2}, \hat{\mu}_j = \frac{c_j}{I_f \Omega}$ for $j = 5, 6, 7$, and

$$\Gamma(\theta) = \sin \theta \left(p_o(\theta) + \frac{p_e(\theta) \cos \theta}{\sqrt{1 - k_1^2 \sin^2 \theta}} \right), \quad (10)$$

$$p_o(\theta) = \frac{P_o(\theta) l_1}{I_f \Omega^2}, \quad p_e(\theta) = \frac{k_1 P_e(\theta) l_1}{I_f \Omega^2}. \quad (11)$$

The transformation of independent variable from τ to θ is possible under the reasonable assumption that $\dot{\theta}$ is always positive, *i.e.*, the engine never reverses direction. The transformation is realized by expressing τ as a function of θ (the solution for this relationship is never actually required in the analysis). Following the nondimensional procedure and the change of independent variable, the final form of the equations of motion is determined to be

$$\begin{aligned} y s_i'' + [s_i' + g_i(s_i)] y' - \frac{1}{2} \frac{dx_i}{ds_i}(s_i) y & \\ = -\hat{\mu}_{ai} s_i', \quad i = 1, \dots, N, & \quad (12) \\ \sum_{i=1}^N b_i \left[\frac{dx_i}{ds_i}(s_i) s_i' y^2 + x_i(s_i) y y' + g_i(s_i) s_i' y y' \right. & \\ \left. + \frac{dg_i}{ds_i}(s_i) s_i'^2 y^2 \right] + g_i(s_i) s_i'' y^2 + b_o(\theta) y y' & \\ = -\frac{1}{2} b_o'(\theta) y^2 + \sum_{i=1}^N b_i \hat{\mu}_{ai} g_i(s_i) s_i' y + \Gamma_o + \Gamma(\theta) & \end{aligned}$$

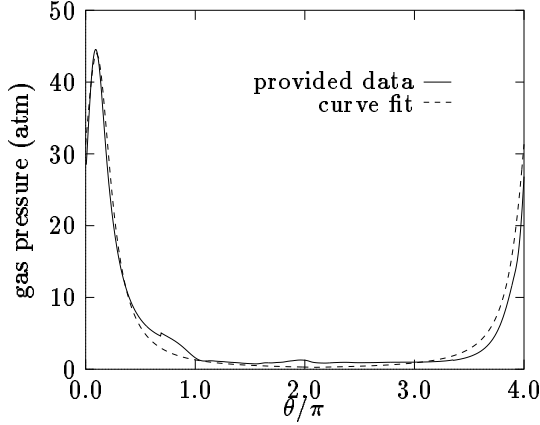


FIGURE 3: GAS PRESSURE DATA FOR A 1.9 L, FOUR-STROKE, FOUR-CYLINDER ENGINE RUNNING AT 1400 RPM WITH BOTH PROVIDED DATA AND A FITTING CURVE. (DATA COURTESY OF PROFESSOR HAROLD SCHOCK, MICHIGAN STATE UNIVERSITY)

$$- \left[\hat{\mu}_5 + \hat{\mu}_7 \sin^2 \theta + \frac{(c_6 + c_7 k_1^2 \sin^2 \theta) \cos^2 \theta}{1 - k_1^2 \sin^2 \theta} \right] y, \quad (13)$$

The sources of speed fluctuation for the engine can be divided into the torques generated by load and gas pressure, $\Gamma_o + \Gamma(\theta)$, by bearing damping,

$$- \left[\hat{\mu}_5 + \hat{\mu}_7 \sin^2 \theta + \frac{(c_6 + c_7 k_1^2 \sin^2 \theta) \cos^2 \theta}{1 - k_1^2 \sin^2 \theta} \right] y, \quad (14)$$

by absorber motion,

$$\sum_{i=1}^N b_i \left[\hat{\mu}_{ai} g_i(s_i) s_i' y - \frac{dx_i}{ds_i}(s_i) s_i' y^2 - x_i(s_i) y y' - g_i(s_i) s_i' y y' - g_i(s_i) s_i'' y^2 - \frac{dg_i}{ds_i}(s_i) s_i'^2 y^2 \right], \quad (15)$$

and by the variation of the moment of inertia of the engine which is equivalent to

$$-\frac{1}{2} b_o'(\theta) y^2. \quad (16)$$

3 CASE STUDIES

The goal of this section is to investigate the effects of various absorber configurations on an in-line, four-stroke, four-cylinder engine. For the cases considered here, the paths for the absorber center of mass are taken to be epicycloids of the form, $x(s) = 1 - K^2 s^2$, where K is the tuning order for the absorber. Three configurations are considered in this study. Configuration (1) utilizes a single absorber tuned with $K = 2$. This represents an attempt to counteract the second order harmonic as suggested by Denman (1992). However, the torque induced by the absorber motion is known to contain higher order harmonics and these may add with the applied torques harmonics and accentuate vibrations at higher orders. Configuration (2) utilizes a pair of absorbers, $N = 2$, both tuned with $K = 1$. These absorbers will generate a purely second order torque when

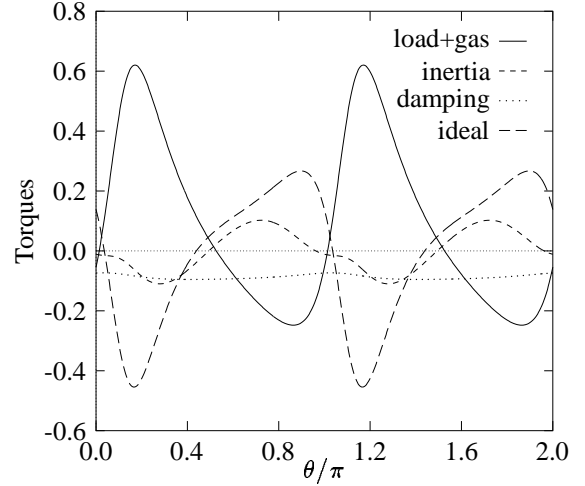


FIGURE 4: TORQUE COMPONENTS OF A 1.9 L, FOUR-STROKE, FOUR-CYLINDER ENGINE; WITHOUT ABSORBERS.

moving in a subharmonic, out-of-phase motion (Lee et al, 1994). Configuration (3) employs two absorbers with $K = 2$ and $K = 4$. This idea, also used by Borowski et al. (1991), is an attempt at confronting the fourth order torques by an additional absorber. While this may appear to be a favorable configuration, the potential trade-off here is that if one must reduce the mass of the $K = 2$ absorber in order to make room for the $K = 4$ absorber, the $K = 2$ absorber will move at a larger amplitude, thereby generating higher harmonic torques which may be only partially counteracted by the $K = 4$ absorber. It should be noted that in typical applications there will be several absorbers tuned to the orders of interest, and it is assumed that each set of absorbers will move appropriately in unison. (Recent simulation studies with multiple absorbers indicates that these motions in unison may become dynamically unstable at moderate torque levels. This is a topic of current research.)

The total moment of inertia of the absorbers is held to be the same for each case. With the minimization of the maximum value of angular acceleration $\ddot{\theta}$ as the goal, it is found that Configuration (3) yields the best result, while Configuration (1) may achieve a worse result than the case in which the absorbers are locked at $s = 0$.

The data for the engine are as follows: $m_{b1} = 0.5$ Kg, $m_{b2} = 0.8$ Kg, $m_p = 0.9$ Kg, $l_1 = 3.97$ cm, $l_2 = 13.22$ cm, and $I_f = 0.05$ Kg-m². The centers of mass of the crank throws and the connecting rods are assumed to be located at their individual mid-points. The total moment of inertia of all absorbers is chosen to be 0.04 Kg-m² in each case, in which the moment of inertia is equally divided for Configurations (2) and (3). The damping levels are assigned as $\hat{\mu}_5 = 0.08$ and $\hat{\mu}_6 = \hat{\mu}_7 = 0.004$, while the absorber damping is $\hat{\mu}_{ai} = 0.005$ in all cases. The gas pressure inside of a cylinder is shown in Figure 3 at $\Omega = 1400$ rpm, where some provided data and a fitted curve are both shown. The empirical formula for the fitting curve is given by

$$P(\theta) = \frac{10.74}{(\theta - 0.314)^2 + 0.244} \text{ (atm)}, \quad (17)$$

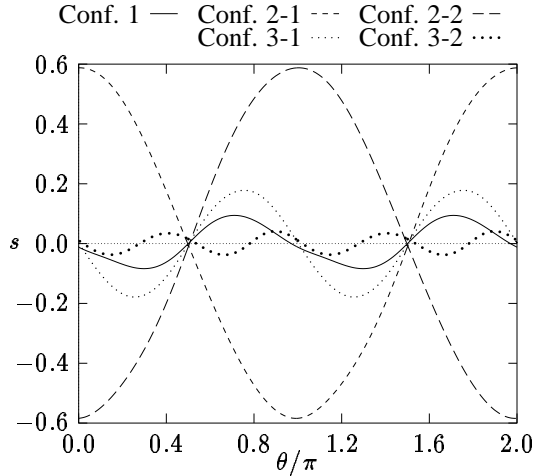


FIGURE 5: ABSORBER MOTIONS FOR CONFIGURATIONS (1)–(3).

in the interval of $-2\pi \leq (\theta - 0.314) \leq 2\pi$. This function is extended to be periodic with a period of 4π , and is then used in numerical simulations. The diameter of the pistons is taken to be 10 cm.

Figure 4 shows the torque curves generated by load and gas pressure, engine inertia, and bearing damping, for the case without absorbers. In Figure 4, the torque curve marked as “ideal” is the ideal torque required from the absorbers such that the engine will run at a constant rate; it is equal to the negative of the sum of the gas pressure torque, the friction torque, and the inertia torque in the steady state case with $y = 1$. Note that the ideal torque has significant levels of higher harmonics.

Figure 5 shows the steady-state absorber motions for Configurations (1)–(3), where the first absorber in Configuration (3) is of second order, and the other is of fourth order. In the figure, “Conf. 2-1” and “Conf. 2-2” denotes the motion of the first and the second absorbers of Configuration (2), respectively, while “Conf. 3-1” and “Conf. 3-2” represent the motion of the $K = 2$ and $K = 4$ absorbers of Configuration (3), respectively. Note that the two absorbers in Configuration (2) move out-of-phase relative to each other and with a period twice that of the excitation torque, which means that they perform their subharmonic motion as expected. Also, note that they undergo large amplitude motions.

The main results are shown in Figures 6 and 7. Figure 6 shows the steady-state angular accelerations of the crankshaft for absorber Configurations (1)–(3), along with those for the case with no absorbers and that with the absorbers locked at their vertices. Figure 7 indicates the torques generated by the absorber systems for the three absorber configurations and with the absorbers locked; the ideal required torque for achieving zero angular acceleration is also shown for reference purposes. It is observed that the simple presence of the absorber inertia reduces the levels of angular acceleration. Configuration (1) actually yields higher angular accelerations than those found for the locked configuration. This is due to the effects of higher order torque harmonics. Configuration (2) reduces the peak angular acceleration by addressing the second order torque,

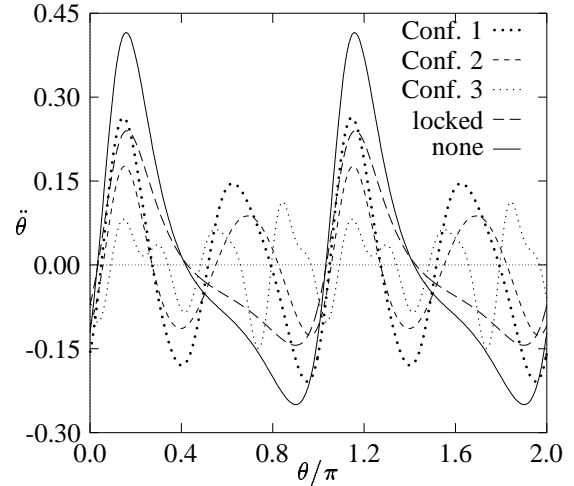


FIGURE 6: CRANKSHAFT ANGULAR ACCELERATIONS FOR CONFIGURATIONS (1)–(3).

but is limited in overall effectiveness since it cannot deal with the higher order torques. Configuration (3) is the most successful, as the $K = 4$ absorber is effective in taking up the vibrations at fourth order, including those induced by the motion of the $K = 2$ absorber. Figure 7 shows that the absorber torque from Configuration (3) does indeed track the ideal torque most closely.

4 DISCUSSION

This preliminary study indicates that for complex periodic torque inputs such as those arising in internal combustion engines, one must employ absorbers tuned to at least two orders in order to achieve satisfactory results. In fact, if one uses absorbers tuned only to the primary harmonic order, the resulting vibrations can in some cases be worse than those encountered with absorbers locked. (This will not generally be the case, however, as absorber systems are designed so as not to increase the total moment of inertia of the engine.) More detailed studies are needed in order to fully appraise the performance of the various absorber configurations. Such investigations are currently underway and will include parameter studies over ranges of operating torques and speeds, more realistic modeling of engine dissipation mechanisms, and usage of other absorber configurations, including multiple pairs of subharmonic absorbers.

REFERENCES

- Borowski, V. J., H. H. Denman, D. L. Cronin, S. W. Shaw, J. P. Hanisko, L. T. Brooks, D. A. Mikulec, W. B. Crum, and M. P. Anderson 1991. Reducing vibration of reciprocating engines with crankshaft pendulum absorbers. SAE Technical Paper Series 911876.
- Cronin, D. L. 1992. Shake reduction in an automobile engine by means of crankshaft-mounted pendulums. *Mechanism and Machine Theory* **27**:517–533.

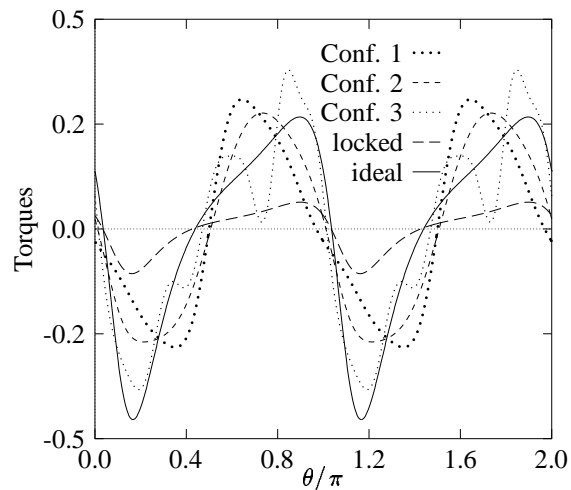


FIGURE 7: ABSORBER TORQUES FOR CONFIGURATIONS (1)–(3), FOR THE ABSORBERS LOCKED, AND THE “IDEAL” TORQUE.

Denman, H. H. 1985. Remarks on brachistochrone–tautochrone problems. *American Journal of Physics* **53**:781–782.

Denman, H. H. 1992. Tautochronic bifilar pendulum torsion absorbers for reciprocating engines. *Journal of Sound and Vibration* **159**:251–277.

Ker Wilson, W. Practical Solution of Torsional Vibration Problems, Volume IV, Chapter XXX, Chapman and Hall Ltd London, 3rd edition, 1968.

Lee, C.-T., S. W. Shaw, and V. T. Coppola 1994. A subharmonic vibration absorber for rotating machinery. *ASME Journal of Vibration and Acoustics*, to appear.

Shaw, S. W. and C.-T. Lee 1994. On the nonlinear dynamics of centrifugal pendulum vibration absorbers. to appear in *Smart Structures, Nonlinear Vibration, and Control*, ed. A. Guran and D. Inman, Chapter VII. Prentice Hall, Inc. New York, N. Y.